Consequences of changes in vegetation and snow cover for climate feedbacks in Alaska and northwest Canada

2016 Environ. Res. Lett. 11 105003

(http://iopscience.iop.org/1748-9326/11/10/105003)

Environmental Research Letters

LETTER

Consequences of changes in vegetation and snow cover for climate feedbacks in Alaska and northwest Canada

E S Euskirchen[1], **A P Bennett**[2], **A L Breen**[2], **H Genet**[1], **M A Lindgren**[2], **T A Kurkowski**[2], **A D McGuire**[3] **and T S Rupp**[2]

[1] University of Alaska Fairbanks, Institute of Arctic Biology, Fairbanks, AK 99775, USA
[2] University of Alaska Fairbanks, International Arctic Research Center, Fairbanks, AK 99775, USA
[3] U.S. Geological Survey, Alaska Cooperative Fish and Wildlife Research Unit, University of Alaska Fairbanks, Fairbanks, AK 99775, USA

E-mail: seeuskirchen@alaska.edu

OPEN ACCESS

RECEIVED
31 March 2016

REVISED
22 August 2016

ACCEPTED FOR PUBLICATION
14 September 2016

PUBLISHED
3 October 2016

Keywords: atmospheric heating, snow cover duration, shrubification, treeline advance, boreal forest fire, tundra fire, carbon storage

Supplementary material for this article is available online

Abstract

Changes in vegetation and snow cover may lead to feedbacks to climate through changes in surface albedo and energy fluxes between the land and atmosphere. In addition to these biogeophysical feedbacks, biogeochemical feedbacks associated with changes in carbon (C) storage in the vegetation and soils may also influence climate. Here, using a transient biogeographic model (ALFRESCO) and an ecosystem model (DOS-TEM), we quantified the biogeophysical feedbacks due to changes in vegetation and snow cover across continuous permafrost to non-permafrost ecosystems in Alaska and northwest Canada. We also computed the changes in carbon storage in this region to provide a general assessment of the direction of the biogeochemical feedback. We considered four ecoregions, or Landscape Conservations Cooperatives (LCCs; including the Arctic, North Pacific, Western Alaska, and Northwest Boreal). We examined the 90 year period from 2010 to 2099 using one future emission scenario (A1B), under outputs from two general circulation models (MPI-ECHAM5 and CCCMA-CGCM3.1). We found that changes in snow cover duration, including both the timing of snowmelt in the spring and snow return in the fall, provided the dominant positive biogeophysical feedback to climate across all LCCs, and was greater for the ECHAM ($+3.1$ W m^{-2} decade^{-1} regionally) compared to the CCCMA ($+1.3$ W m^{-2} decade^{-1} regionally) scenario due to an increase in loss of snow cover in the ECHAM scenario. The greatest overall negative feedback to climate from changes in vegetation cover was due to fire in spruce forests in the Northwest Boreal LCC and fire in shrub tundra in the Western LCC (-0.2 to -0.3 W m^{-2} decade^{-1}). With the larger positive feedbacks associated with reductions in snow cover compared to the smaller negative feedbacks associated with shifts in vegetation, the feedback to climate warming was positive (total feedback of $+2.7$ W m^{-2} decade regionally in the ECHAM scenario compared to $+0.76$ W m^{-2} decade regionally in the CCCMA scenario). Overall, increases in C storage in the vegetation and soils across the study region would act as a negative feedback to climate. By exploring these feedbacks to climate, we can reach a more integrated understanding of the manner in which climate change may impact interactions between high-latitude ecosystems and the global climate system.

Introduction

Although climate is the dominant control on the spatial distribution of vegetation communities, vegetation may in turn feedback to influence the climate. This feedback may be through biophysical factors such as changes in albedo and energy exchange, or biogeochemical factors, such as changes in carbon (C) cycling (Bonan 2008). In particular, it has been well documented that changes in arctic and boreal vegetation can feedback to influence the climate system (Eugster *et al* 2000, Chapin *et al* 2005, Euskirchen *et al* 2010, Shuman *et al* 2011).

In the boreal and arctic ecosystems of Alaska and northwest Canada, recent vegetation shifts are attributed to dynamics that include treeline migration (latitudinal and elevational), greater shrub cover in the tundra, reduced growth of spruce forests under drought stress, and disturbances such as fire. Each of these shifts may alter the reflectance, energy balance, and carbon cycling of a given ecosystem, resulting in a climate feedback, both regionally (Chapin *et al* 2005, Euskirchen *et al* 2009a), or even globally (Betts 2000, Sturm *et al* 2005). In this region, latitudinal treeline is mapped as the limit of white spruce (*Picea glauca*) along the south slope of the Brooks Range in Alaska, whereas elevational treeline is mapped for each of the other mountain ranges, ranging from near sea level in western Alaska to approximately 1250 m in the eastern interior (Viereck 1979). In recent decades, both latitudinal and elevational treeline advance in Alaska have been documented (Viereck 1979, Suarez *et al* 1999, Lloyd 2005). However, studies have also documented reduced growth of both low elevation and treeline white spruce forests due to temperature-induced drought stress (Barber *et al* 2000, Wilmking *et al* 2004) or other factors (Brownlee *et al* 2016). The lower albedo and greater sensible heat flux of forests compared to tundra suggests that northward forest expansion could be a positive biogeophysical feedback to regional warming (de Wit *et al* 2014), although reduced growth may result in higher albedo, serving as a negative biogeophysical feedback. In concert with changes in treeline, other studies have documented a shrubification of the tundra, including increases in the biomass and abundance of shrubs (Tape *et al* 2006, Myers-Smith *et al* 2015). An increase in shrub abundance in the tundra, accompanied by a lower albedo and greater sensible heat flux, may also act as a positive biogeophysical feedback to warming (McFadden and Chapin 1998, Lynch *et al* 1999, Chapin *et al* 2000, Euskirchen *et al* 2009b, Loranty *et al* 2011, Bonfils *et al* 2012).

Wildfire is the dominant disturbance regime of the boreal forests in Alaska and northwest Canada, with generally short fire return intervals of 50–150 years (Payette 1992). This creates a mosaic of stand ages across the region, with each forest stand representing a specific post-fire successional stage. Concurrent with hotter, drier conditions, an increased frequency of years with large fires from the 1960s to the 2000s has tripled the area burned in the North American boreal forest region (Duffy *et al* 2005, Kasischke 2010, Calef *et al* 2015). This leads to a landscape with a large proportion of young deciduous stands, which have a greater albedo than mature coniferous forests, resulting in a negative biogeophysical feedback to climate warming. Research also suggests that warmer and drier summers in areas covered by tundra may also experience more burning, with climate change projections suggesting that the area burned in tundra will double by the end of this century (Hu *et al* 2015).

Furthermore, in these high-latitude regions, as temperatures warm, the duration of the snow covered period is reduced, in terms of both an earlier melt in the spring and a later return in the fall (Callaghan *et al* 2011 and references therein). These decreases in the duration of snow cover result in greater amounts of absorbed solar radiation and a positive feedback to climate warming, in what is commonly known as the snow-albedo feedback loop. Changes in vegetation may interact with changes in snow cover to moderate this snow-albedo feedback loop. For example, as the amount of annual area burned increases, treeless areas, which have a particularly high reflectance when covered with snow, replace forests in the first years following fire, and can thus act to cool the climate (Randerson *et al* 2006).

In concert with these biogeophysical feedbacks to climate associated with shifts in vegetation and snow cover, we expect biogeochemical feedbacks associated with changes in carbon stored in the soils and vegetation. Permafrost ecosystems store large amounts of soil organic C in the first several meters of the permafrost because decomposition rates are low in these cold, often wet soils (Hugelius *et al* 2014). Under a warming climate, thawing of additional upper permafrost layers adds soil organic C to the active layer, thereby increasing the pool of decomposable soil organic matter. This pool is labile and could become available for microbial degradation as the active layer continues to deepen (Mueller *et al* 2015), with fire occurrence potentially adding to this loss of soil C (Mack *et al* 2011, Turetsky *et al* 2015). Plant productivity may increase under warmer temperatures thereby sequestering more C (Shaver *et al* 1991, Natali *et al* 2012) or it may decrease due to fire and drought stress thereby releasing more C (Beck *et al* 2011). Storage in soil C pools may also increase with greater inputs from increased plant growth (Gorham 1991, Hobbie 1996). Consequently, although soil C pools may decrease under warmer temperatures through soil organic matter decomposition and combustion during fire, this may be compensated by greater inputs from plants. Thus, the net C balance of these ecosystems will be controlled by the balance between potential changes in plant productivity and release of C from soils.

In previous work, we examined energy feedbacks to climate due to changes in: (1) snow cover at the pan-Arctic scale (Euskirchen *et al* 2007), (2) both snow cover and vegetation due to shifts in the fire regime across boreal Alaska and northwest Canada (Euskirchen *et al* 2009a) and, (3) increased shrub growth (but not changes in distribution) and changes in snow cover in arctic Alaska (Euskirchen *et al* 2009b). Our previous work (Chapin *et al* 2005, Euskirchen *et al* 2009a, 2009b) has shown that in arctic and boreal ecosystems, changes in snow cover exert a stronger feedback to warming than shifts in vegetation type. The work presented here builds on these studies by including a more comprehensive suite of the types

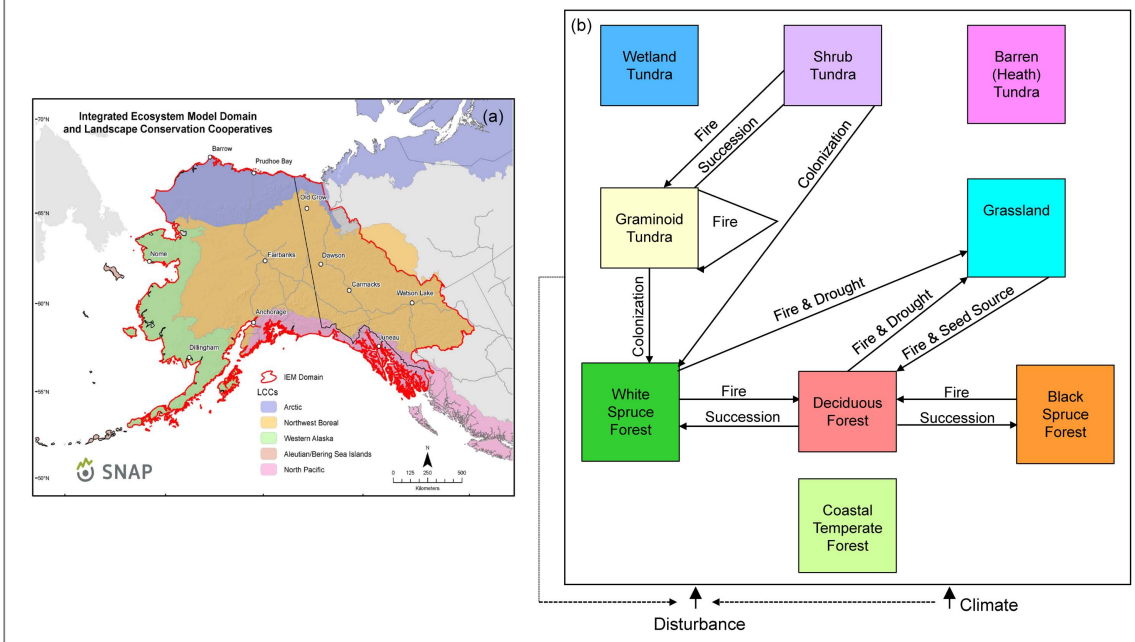

Figure 1. Map of the study area and conceptual diagram of the ALFRESCO model. In (a), the study region in Alaska and northwest Canada depicting the Landscape Conservation Cooperatives (LCCs) that are considered here, including the Arctic, Northwest Boreal, Western Alaska and North Pacific LCCs. Not considered is the Aleutian Bering Sea Islands LCC due to its maritime focus. In (b), a conceptual diagram of the ALFRESCO model illustrating the vegetation types represented in this study and their pathways of change. A one-way arrow indicates that the vegetation transition is one-way. Vegetation types that do not include arrows remain static.

of vegetation change, including changes in shrub distribution and growth, tundra fires (in addition to boreal fires), advances in treeline, and reduction in forest cover due to drought. We also take a detailed, comparative approach in this study focusing on four distinct ecoregions, or Landscape Conservation Cooperatives (LCCs; Millard *et al* 2012), in Alaska and western Canada: the Western Alaska LCC, the portion of the Arctic LCC in Alaska and northwest Canada, most of the Northwest Boreal LCC except for some area in the Northwest Territories, and the portion of the North Pacific LCC in Alaska (figure 1(a)). It is important to be able to quantify these feedbacks both spatially and temporally since they occur at differing spatial and temporal resolutions. Specifically, the objectives of this study are to project and quantify biogeophysical feedbacks to climate across these four LCCs for the 90 years from 2010 to 2099 due to: (1) vegetation changes from the abundance of shrubs in the tundra, boreal and tundra fire regimes, latitudinal and elevational treelines, and drought stress, and (2) the timing of snow melt in the spring, snow return in the fall and snow cover duration. We also examine the changes in carbon storage of the vegetation and soils of these ecosystems and provide a general direction of the biogeochemical feedbacks to climate based on these changes in carbon storage. We hypothesized that, even after accounting for additional biogeophysical feedbacks not previously considered, decreases in snow cover would remain the dominant positive feedback to climate warming, and that this positive feedbacks would likely be larger than any negative feedbacks associated with greater early successional forests under a heightened fire regime.

Methods

Overview

We performed model simulations for 1900–2100 at a 1 km^2 spatial resolution across Alaska and western Canada, and analyzed the outputs for the 90 years between 2010 and 2099. We used a transient landscape-level model of vegetation and fire dynamics, the Alaskan Frame-based Ecosystem Code (ALFRESCO), to estimate the changes in vegetation dynamics associated with: (1) post-fire distribution of the ages of the ecosystems, (2) treeline, and (3) shrubification of the tundra. We used the Terrestrial Ecosystem Model (TEM) to calculate changes in the length of the snow season, incoming solar irradiance and longwave radiation, and changes in vegetation and soil C. We then computed changes in atmospheric heating across the study region due to projected changes in vegetation dynamics, the length of the snow season, and C storage. Below, we provide further details of the study region, the ALFRESCO and TEM models, model input datasets, and calculations of atmospheric heating.

Study region and vegetation map

Our study region focuses on four Landscape Conservation Cooperatives (LCCs; Millard *et al* 2012) in Alaska and northwest Canada including the Western Alaska LCC and parts of the Arctic, Northwest Boreal, and North Pacific LCCs (figure 1(a)). For simplicity,

we refer to these as the Western Alaska, Arctic, Northwest Boreal, and North Pacific LCCs throughout the rest of this paper. These four LCCs correspond to the major ecoregions in Alaska and northwest Canada. To simulate plant growth and treeline dynamics, vegetation composition and distribution, wildfire, and biogeochemistry across the landscape, we relied on a baseline vegetation map of our study region. This map included information from the North American Land Change Monitoring System 2005 dataset (for arctic and subarctic ecosystem types) and the National Land Cover Dataset 2001 (for coastal temperate rainforest ecosystem types), the only two presently available maps with region-wide data for this study.

This vegetation map permitted us to classify the major vegetation types in our study region by LCC, including black and white spruce forest, deciduous forests, maritime coastal temperate forests, heath tundra, shrub tundra, graminoid (tussock) tundra, and wetland (wet sedge) tundra. Although further details of this classification are available in Zhu and McGuire (2016, chapter 2), here we provide an overview of the vegetation composition in each LCC.

The Arctic LCC contains all four types of tundra, with the dominant tundra types relatively evenly distributed between shrub and graminoid tundra, 108 226 km^2 and 119 027 km^2 respectively (Zhu and McGuire 2016, chapter 2). There were minor components of deciduous forest, and white and black spruce forests, primarily distributed near the southern border of the Arctic LCC, which generally corresponds to latitudinal treeline. The Northwest Boreal LCC consists primarily of deciduous forest (305 051 km^2, where the 'deciduous' category consists of both pure deciduous and mixed deciduous-spruce forests), with substantial coverage of pure white spruce forest (120 395 km^2) and black spruce forest (88 995 km^2), and minor components of all tundra types. The North Pacific LCC is dominated by maritime coastal temperate forest (76 000 km^2), and small components of deciduous, white spruce, and black spruce forests. The Western Alaska LCC is relatively evenly dominated by deciduous forest (130 904 km^2) and shrub tundra (119 517 km^2), with small components of graminoid tundra, and white and black spruce forests. Although we do not explicitly include wetlands, the simulations with TEM (described below) include separate calibrations for three upland and lowland forest types (black spruce, white spruce, and deciduous forests), with lowland vegetation in the black spruce boreal ecosystems generally corresponding to wetlands, while graminoid and wet sedge tundra correspond to wetlands in the tundra ecosystems.

ALFRESCO model

We used a transient, biogeographic model, ALFRESCO (figure 1(b); e.g., Rupp *et al* 2000, Johnstone *et al* 2011, Gustine *et al* 2014, Hewitt *et al* 2015), to simulate changes in vegetation type due to fire disturbance, natural succession, treeline advance, and shrubification from 2010 to 2100. This model includes the dominant vegetation types of Alaska and northwest Canada as described above, including black spruce forests, white spruce forests, deciduous forests, heath (barren lichen-moss) tundra, shrub tundra, wetland (wet sedge) tundra, graminoid (tussock) tundra, and maritime coastal temperate forests. The heath tundra, wetland tundra, and maritime forests are currently treated as static vegetation states in the model.

The fire module of ALFRESCO uses a cellular automata approach with separate subroutines for cell ignition and spread to simulate annual fire season activity, where additional details on the fire module are provided in Zhu and McGuire (2016, chapter 2). Following a wildfire, burned spruce forest (white or black) transitions into early successional deciduous forest, while burned deciduous forest self-replaces (figure 1(b)). Transitions in tundra are due to succession or colonization and infilling. These tundra transitions are influenced by climate and fire history, which in turn are influenced by proximity to seed source, seedling establishment and growth conditions. For the transition from tundra to forest at treeline, seed dispersal occurs within a 1 km^2 neighborhood. White spruce colonization/infilling may occur in both graminoid and shrub tundra with transition rates to spruce forest regulated by climate effects and basal area growth accrual. Drought stress may also influence treeline and vegetation shifts, and is modeled in ALFRESCO based on temperature and precipitation thresholds. Vegetation succession from graminoid to shrub tundra is modeled probabilistically, with a greater likelihood of transition to shrub tundra post-fire. When fires occur in the tundra, shrub tundra transitions to graminoid tundra, and while graminoid tundra is self-replacing (figure 1(b)). Vegetation transitions, defined as at least one shift in vegetation type during the projection period (2010–2099), were calculated as a percent of total area for each of the four LCC subregions. Although a grid cell generally cannot contain a fraction of a vegetation type, there may be an accumulation of white spruce basal area in tundra cells prior to transition to white spruce once the basal areal threshold has been reached. Furthermore, even though ALFRESCO uses an input vegetation map, the model is robust to initialization conditions. The map is used only at the beginning of a 1000 year model spin-up, with random age classes distributed over the landscape, across 200 model simulation replicates. This results in a rapidly converging ratio of vegetation types on the landscape by present time, with additional details provided in Mann *et al* (2012). The original 'mixed' class was reclassified as deciduous in the initialization vegetation map and the model only considers 'Deciduous or 'Black' or 'White' Spruce. Age is the key factor in determining the transition between 'Deciduous' or 'Black' or 'White' Spruce, and stands

that are on the border between age thresholds could be considered 'Mixed', but this is presently not represented in the model. Depending on the age class of a given pixel, the associated probability of burning (cell ignition) is adjusted. The probability of a cell igniting and fire spreading to neighboring cells is also related to temperature and precipitation as well as vegetation type.

TEM with a dynamic organic soil module (DOS-TEM)

We implemented a linear coupling between ALFRESCO and TEM, allowing for the exchange of information between the models to occur in series. Here, the spatially-explicit time series of fire occurrence simulated by ALFRESCO is used to drive the process-based TEM with a Dynamic Organic Soil Module (DOS-TEM; Raich *et al* 1991, Yi *et al* 2010, Genet *et al* 2013). DOS-TEM then simulates the effects of wildfire, warming, and historical logging on carbon pools and aerobic carbon processes. DOS-TEM has been extensively used in arctic and boreal regions, with applications to the soil environment (e.g., Zhung *et al* 2001, 2003, Yi *et al* 2010), fire (e.g., Balshi *et al* 2009), and interactions between fire and carbon storage (Genet *et al* 2013). Although DOS-TEM has been extensively described in these studies, and most recently in Zhu and McGuire (2016), we briefly describe the model here. DOS-TEM belongs to the TEM family of process-based ecosystem models that are designed to simulate carbon and nitrogen pools of the vegetation and the soil, and carbon and nitrogen fluxes among vegetation, soil, and the atmosphere (Raich *et al* 1991, McGuire *et al* 1992). DOS-TEM is comprised of four modules: an environmental module, an ecological module, a disturbance module and a dynamic organic soil module. The environmental module simulates the dynamics of biophysical processes in the soil and the atmosphere, including soil temperature (including permafrost dynamics) and moisture conditions for multiple layers within various soil horizons including moss, fibric and humic organic horizons, and mineral horizons. The ecological module simulates carbon and nitrogen dynamics in the atmosphere, vegetation, and soil, while the dynamic organic soil layer module calculates thickness of the fibric and the humic organic layers, after soil carbon pools are altered by ecological processes (litterfall, decomposition and burial) and fire disturbance. The disturbance module simulates the effects of logging and wildfire on soil and vegetation carbon and nitrogen pools, taking into account the C lost to combustion during wildfires as described in Yuan *et al* (2012) and Genet *et al* (2013). For wildfire, the module computes combustion emissions to the atmosphere, the fate of un-combusted C and N pools, and the flux of N from the atmosphere to the soil via biological N fixation in the years following fire. In boreal forest, the amount of soil C combusted during a wildfire is determined using input data on topography, drainage, and vegetation, as well as soil (moisture and temperature) and atmospheric (evapotranspiration) environmental data (Genet *et al* 2013). In tundra, the rates of combustion are based on estimates from the 2007 Anaktuvuk River Fire (Mack *et al* 2011).

DOS-TEM takes as inputs information pertaining to climate (monthly mean air temperature, total precipitation, net incoming shortwave radiation and vapor pressure, which is converted to vapor pressure deficit in the environmental module), drainage, soil texture, elevation, and vegetation type. The model is calibrated by vegetation type for rate-limiting parameters represented in the model based on target values of C and N pools and fluxes of representative mature ecosystems. These parameters were 'tuned' until the model reached target values of the main C and N pools and fluxes (Clein *et al* 2002). For boreal forest communities, an existing set of target values for vegetation and soil carbon and nitrogen pools and fluxes was assembled using data collected in the Bonanza Creek Long Term Ecological Research (LTER) program (Yuan *et al* 2012). For the tundra communities, we used data collected at the Toolik Field Station (Shaver and Chapin 1991, Van Wijk *et al* 2003, Sullivan *et al* 2007, Euskirchen *et al* 2012, Gough *et al* 2012, Sistla *et al* 2013). Finally, for the maritime upland forest, we used data collected from a long-term carbon flux study in the North American Carbon Program (D'Amore *et al* 2012). The target values for maritime alder shrubland were assembled from Binkley (1982).

As described in Zhu and McGuire (2016, chapter 6), the model has been validated by comparing simulated soil and vegetation carbon stocks with field observations, including soil observations from the National Soil Carbon Network database (Johnson *et al* 2011) and vegetation biomass estimates from the Arctic LTER database (http://toolik.alaska.edu) for shrub, tussock, wet sedge, and heath tundra as well as forest inventory data collected by the Cooperative Alaska Forest Inventory for upland and lowland black spruce, white spruce and deciduous forest (Malone *et al* 2009). In terms of the validation of the other modules of DOS-TEM, regional applications of this model in northern high latitudes have included validation at seasonal to century scales for processes related to soil thermal activity (Zhuang *et al* 2001, 2003a, 2003b), snow cover (Euskirchen *et al* 2006, 2007), and fire (Balshi *et al* 2009, Yuan *et al* 2012, Genet *et al* 2013).

In this application, the biogeochemical outputs of interest include vegetation C stock estimates, derived from the sum of the above- and belowground living biomass, and soil C stocks. Soil C stocks are composed of carbon stored in the dead woody debris fallen to the ground, moss horizon, organic soil horizons, and mineral soil horizons. We computed regional area-weighted estimates of the vegetation and soil C pools in two ways: (1) by taking into account changes in the

area of a given vegetation type, as derived in ALFRESCO, and (2) by assuming the area of each vegetation type remained constant to that in the first decade of the analysis, thereby permitting us to generally understand the impact of changes in vegetation on changes in C pools.

We use the environmental module of DOS-TEM to estimate the changes in the timing of snowmelt, snow return, and the duration of the snow season with methodology previously implemented in Euskirchen *et al* (2006, 2007, 2009a, 2009b). Snow pack accumulates whenever mean monthly temperature is below −1 °C, and snow melt occurs at or above −1 °C. At elevations of 500 m or less, the model removes the entire snow pack, plus any new snow by the end of the first month with temperatures above −1 °C. At elevations above 500 m, the melting process requires 2 months above −1 °C, with half of the first month's snow pack retained to melt during the second month. We incorporate an algorithm to estimate the date of snowmelt (or snow return) from the monthly estimates of snowpack. This algorithm uses a 'ramp' between monthly temperatures (Euskirchen *et al* 2007). Linear interpolations of data for monthly air temperature and the month(s) preceding snowmelt (or snow return), the month of snowmelt (or snow return), and the month following snowmelt (or snow return) are performed. For example, to calculate the date of snowmelt when all snow has disappeared by April, approximately 30 points are interpolated between mean monthly March and April air temperature to determine the 15 points for the first half of April and approximately 30 points are interpolated between mean monthly air temperature in April and May to determine the 15 points for the second half of April. The length of the snow-free season is calculated by subtracting the Julian date of snowmelt from the Julian date of snow return. To examine changes in the timing of snowmelt, snow return and snow cover duration between 2010 and 2099, we calculated anomalies based on the mean day of snow melt, snow return and number of days of snow cover duration for the period from 1980 to 2009. We calculate the anomaly for a given decade based on the difference between the day of snowmelt/return or total snow duration for a given decade from 2010 to 2099 minus mean day of snowmelt/return or total duration in the 30 years preceding the prognostic simulations, from 1980 to 2009. As discussed in Euskirchen *et al* (2006, 2007), the model estimates of the spatial extent and the temporal dynamics of snow cover are in agreement with those of Dye (2002).

Climate data

The baseline period for both the ALFRESCO and TEM simulations was defined as the period from 1950–2009. This period corresponds to the beginning of reliable wildfire observations and statistics for this region (1950) and the end of contemporary downscaled historic climate observations (2009). The projection period was defined as the period from 2010 to 2099. Although the climate inputs to ALFRESCO include air temperature and precipitation, those for TEM include air temperature and precipitation as well as downwelling surface radiation and vapor pressure. Below, we describe the climate datasets and downscaling methods.

Historical (Climate Research Unit—CRU TS 3.1; Harris *et al* 2014) and projected (CMIP3) output variables of surface temperature (°C), precipitation (mm), and cloudiness (%) were downscaled via the delta method (Hay *et al* 2000, Hayhoe 2010) using PRISM 1961–1990 2 km resolution climate normals as baseline climate (Daly *et al* 2008). The delta method was implemented by calculating climate anomalies applied as differences for temperature or quotients for precipitation between monthly future CMIP3 data and calculated CRU climate normals for 1961–1990 (see http://www.snap.uaf.edu for data and details). These coarse resolution anomalies were then interpolated to PRISM spatial resolution via a spline technique, and then added to (temperature, downwelling radiation) or multiplied by (precipitation) the PRISM climate normals. The downscaled climate data were then bias corrected to account for mismatches between the historical and future data, and interpolated to a 1 km^2 resolution for modeling purposes.

Monthly surface downwelling shortwave radiation (R_{Sin}, MJ m^{-2} d^{-1}) is calculated for use in TEM and for calculating changes in atmospheric heating. The algorithm takes into account the downscaled cloudiness data (as described above) and the baseline climatology global irradiance (GIRR, monthly, MJ m^{-2} d^{-1}) to calculate R_{Sin} based on an equation from Allen *et al* (1998) at a monthly time step and 1 km^2 spatial scale:

$$R_{Sin} = GIRR * \{0.251 + (0.509 * (1.0 - cloudiness/100))\}. \quad (1)$$

Values of longwave radiation (W m^{-2}) are calculated, including incoming longwave radiation (R_{Lin}), outgoing longwave radiation (R_{Lout}), and net longwave radiation (R_{Lnet}), based on Idso and Jackson (1969), and include a cloud correction factor (Parkinson and Washington 1979). The incoming longwave radiation is calculated as:

$$R_{Lin} = \sigma T_a^4 \{1 - 0.26 \exp[-7.77 \times 10^{-4}(273 - T_a)^2]\}. \quad (2)$$

This is modified by the cloud correction factor of $1 + cn$, where c is the fractional cloud cover value and n is an empirical factor set at 0.275 (Parkinson and Washington 1979). The Stefan–Boltzmann constant (σ) = 5.67×10^{-8} W m^{-2} K^{-4}. T is air surface temperature in K.

The outgoing longwave radiation is calculated taking into account the vegetation type and the emissivity values (ε) for the given snow and non-snow covered

vegetation type (Geiger *et al* 2009), in addition to the ground surface temperature (T_g) and the Stefan–Boltzmann law

$$R_{Lout} = \varepsilon\sigma T_g^4 + R_{Lin}(1 - \varepsilon). \quad (3)$$

The net longwave radiation is then calculated by subtracting R_{Lin} from R_{Lout}. This value is typically negative because the thermal radiative temperature of the atmosphere viewed from the air is cooler than the ground surface temperature (Betts and Ball 1997).

We selected two general circulations models (GCMs) of the best performing subset models for Alaska (Walsh *et al* 2008), which bound the climate scenarios from most warming and fire activity (the version 5 of the European Center Hamburg Model from the Max Planck Institute ECHAM5; Roeckner *et al* 2003, 2004) to least warming and more moderate fire activity (the Canadian Center for Climate Modeling General Circulation Model, CCCMA; McFarlane *et al* 1992, Flato 2005). Our analysis focused on a moderate forcing emission scenario (A1B) for the two GCMs from the Intergovernmental Panel on Climate Change's Special Report on Emission Scenarios (IPCC-SRES; Nakicenovic and Swart 2000). We chose only this one scenario due to the computational complexity and associated long run times with DOS-TEM. The AIB emissions scenario is a conservative choice given that global emissions more closely track the A2 scenario (Peters *et al* 2012, IPCC 2013), but we did not want to overestimate the amount of land area burned. Further, since we are using just this one emission scenario, we chose to bracket the variability across two bounding GCMs, choosing the CCCMA and ECHAM from a suite of GCMs, after ALFRESCO simulations indicated maximum (ECHAM) and minimum (CCCMA) area burned across the study domain with these two GCMs under the A1B scenario. We analyzed the climate data for the periods from: September–October (the fall shoulder season), November–March (the cold season), April–May (the spring shoulder season), and June–August (summer).

Methodology for computing atmospheric heating

We assessed potential changes in atmospheric heating and feedbacks to climate due to both changes in vegetation following fire, treeline advance, and shrubification and changes in the snow season. Our calculations of atmospheric heating follow the methodology of Chapin *et al* (2005) and Euskirchen *et al* (2007, 2009a, 2009b), and are described below.

We first compiled information on albedo (α), latent (LE) and sensible heat (H) fluxes for the dominant vegetation types in our region (table 1). These parameterization sites were eddy covariance sites that collected information on the energy fluxes as well as meteorological variables, including both albedo and snow depth. We distinguished between four distinct periods based on the state of the snow cover as seen in the data: pre-snowmelt (six weeks prior to the final snowmelt, generally from March through mid-April for the boreal ecosystems and from early May to early June for the tundra ecosystems), post-snowmelt (mid-April through late August for the boreal ecosystems and from early June through mid-August for the tundra ecosystems), pre-snow return (six weeks prior to consistently snow covered ground, late August–mid October for the boreal ecosystems and mid-August–mid-September for the tundra ecosystems), and post-snow return (mid-October–early March for the boreal ecosystems and mid-September–early May for the tundra ecosytems).

Based on each period of snow cover and each value of albedo obtained from the field data and R_{Sin} obtained from (equation (1)), we calculated outgoing shortwave solar radiation (R_{Sout}) as:

$$R_{Sout} = R_{Sin} * \alpha. \quad (4)$$

Shortwave net radiation (R_{Snet}) is then calculated as the difference between R_{Sin} and R_{Sout}:

$$R_{Snet} = R_{Sin} - R_{Sout}. \quad (5)$$

Seasonal atmospheric heating is then computed by multiplying incoming shortwave and longwave radiation by the proportion of incoming shortwave that is absorbed by the land surface times the proportion of net shortwave that is transferred to the atmosphere minus the absorbed and emitted longwave radiation (R_{Lnet}):

$$\{R_{Sin} + R_{Lin}\} \times \left\{\frac{R_{Snet}}{R_{Sin} + R_{Lin}}\right\} \times \left\{\frac{H + LE}{R_{Snet}}\right\} - R_{Lnet}. \quad (6)$$

Note that the ratios in this calculation are key, in that the terms described collapse into $(\{H + LE\} - R_{Lnet})$, but we have used the ratios to derive $H + LE$. We estimated changes in atmospheric heating due to changes in the length of the snow season, in terms of both snowmelt in the spring and snow return in the fall. We use DOS-TEM-derived values of R_{Sin} and literature-derived values of heat fluxes (table 1) and calculate atmospheric heating for pre- and post-snowmelt based on equation (6). We then compare pre- and post-snowmelt and pre- and post-snow return energy budgets to estimate the changes in snowmelt and snow return on atmospheric heating: {[Daily atmospheric heating post-snowmelt (or pre-snow return)] – [Daily atmospheric heating pre-snowmelt (or post-snow return)]} × [Change in snow cover duration], where the daily atmospheric heating is in units of MJ m^{-2} d^{-1} and the change in snow cover duration is in days yr^{-1}. The estimates of heating are then averaged over the length of the snow-free season, as calculated in the water balance model of DOS-TEM. Estimates of atmospheric heating are presented at the decadal time scale in W m^{-2} based on the mean annual changes in the surface energy flux. Due to the computational complexity and large data files associated with the 1 km^2 model simulations in

Table 1. Mean values of energy budget parameters across the dynamic vegetation types modeled in this study. We also include, for comparison, parameters for a boreal thermokarst collapse scar bog and moderate rich fen. Atmospheric heating is given both as a percentage of long- and shortwave net radiation (% of $R_{Snet} + R_{Lnet}$), calculated based on measured heat flux to the atmosphere [sensible (H) plus latent (LE) fluxes], and in MJ m^{-2} d^{-1}, calculated as in equation (7). Estimated values of albedo (α), H, and LE are obtained from the references. R_{Sin}, incoming shortwave radiation; R_{Lin}, incoming longwave radiation; R_{Snet}, net shortwave radiation; R_{Lnet}, net longwave radiation.

Vegetation type	Reference	Radiation or energy budget parameter	Pre-snowmelt	Post-snowmelt	Pre-snow return	Post-snow return
Boreal evergreen	Euskirchen *et al* (2014)	α	0.40	0.09	0.12	0.41
		$R_{Snet} + R_{Lnet}$ (% of $R_{Sin} + R_{Lin}$)	7	21	16	6
		Atmospheric Heating:				
		(% of $R_{Snet} + R_{Lnet}$)	38	63	44	−6
		MJ m^{-2} d^{-1}	3.9	10.5	6.4	−0.5
Boreal early successional deciduous forest	Amiro *et al* (2006), Liu and Randerson (2008)	α	0.55	0.15	0.15	0.55
		$R_{Snet} + R_{Lnet}$ (% of $R_{Sin} + R_{Lin}$)	10	17	12	−2
		Atmospheric Heating:				
		(% of $R_{Snet} + R_{Lnet}$)	28	68	19	−12
		MJ m^{-2} d^{-1}	2.1	8.2	2.5	−1.4
Boreal grass/shrub/early deciduous, 5 yr post-burn	Amiro *et al* (2006), Liu and Randerson (2008)	α	0.48	0.13	0.24	0.46
		$R_{Snet} + R_{Lnet}$ (% of $R_{Sin} + R_{Lin}$)	11	26	13	6
		Atmospheric Heating:				
		(% of $R_{Snet} + R_{Lnet}$)	30	57	40	−10
		MJ m^{-2} d^{-1}	2.4	7.0	3.3	−1.1
Graminoid tundra	Euskirchen *et al* (2012)	α	0.68	0.24	0.31	0.50
		$R_{Snet} + R_{Lnet}$ (% of $R_{Sin} + R_{Lin}$)	5	21	17	−0.1
		Atmospheric Heating:				
		(% of $R_{Snet} + R_{Lnet}$)	−1	18	11	−3
		MJ m^{-2} d^{-1}	−0.3	6.9	3.3	−0.7
Barren/lichen/moss (heath) tundra	Euskirchen *et al* (2012)	α	0.73	0.27	0.25	0.57
		$R_{Snet} + R_{Lnet}$ (% of $R_{Sin} + R_{Lin}$)	1	18	15	0
		Atmospheric Heating:				
		(% of $R_{Snet} + R_{Lnet}$)	−3	16	11	−12
		MJ m^{-2} d^{-1}	−0.7	1.9	2.8	−1.5
Shrub tundra	Euskirchen *et al* unpublished data	α	0.54	0.24	0.26	0.49
		$R_{Snet} + R_{Lnet}$ (% of $R_{Sin} + R_{Lin}$)	2	14	20	1
		Atmospheric Heating:				
		(% of $R_{Snet} + R_{Lnet}$)	6	20	12	3
		MJ m^{-2} d^{-1}	1.8	7.3	3.6	0.2

Table 1. (Continued.)

Vegetation type	Reference	Radiation or energy budget parameter	Pre-snowmelt	Post-snowmelt	Pre-snow return	Post-snow return
Wet sedge tundra	Euskirchen *et al* (2012)	α	0.73	0.25	0.25	0.51
		$R_{Snet} + R_{Lnet}$ (% of $R_{Sin} + R_{Lin}$)	1	20	16	1
		Atmospheric Heating:				
		(% of $R_{snet} + R_{Lnet}$)	−5	60	46	−4
		MJ m^{-2} d^{-1}	−1.0	6.2	2.9	−0.9
Boreal collapse scar bog	Euskirchen *et al* (2014)	α	0.52	0.17	0.14	0.47
		$R_{Snet} + R_{Lnet}$ (% of $R_{Sin} + R_{Lin}$)	9	24	16	5
		Atmospheric Heating:				
		(% of $R_{Snet} + R_{Lnet}$)	−11	53	36	−26
		MJ m^{-2} d^{-1}	−0.3	6.6	2.1	−1.7
Boreal fen	Euskirchen *et al* (2014)	α	0.69	0.23	0.19	0.49
		$R_{Snet} + R_{Lnet}$ (% of $R_{Sin} + R_{Lin}$)	4	20	14	2
		Atmospheric Heating:				
		(% of $R_{Snet} + R_{Lnet}$)	−13	51	34	−15
		MJ m^{-2} d^{-1}	−0.8	6.0	1.8	−1.9

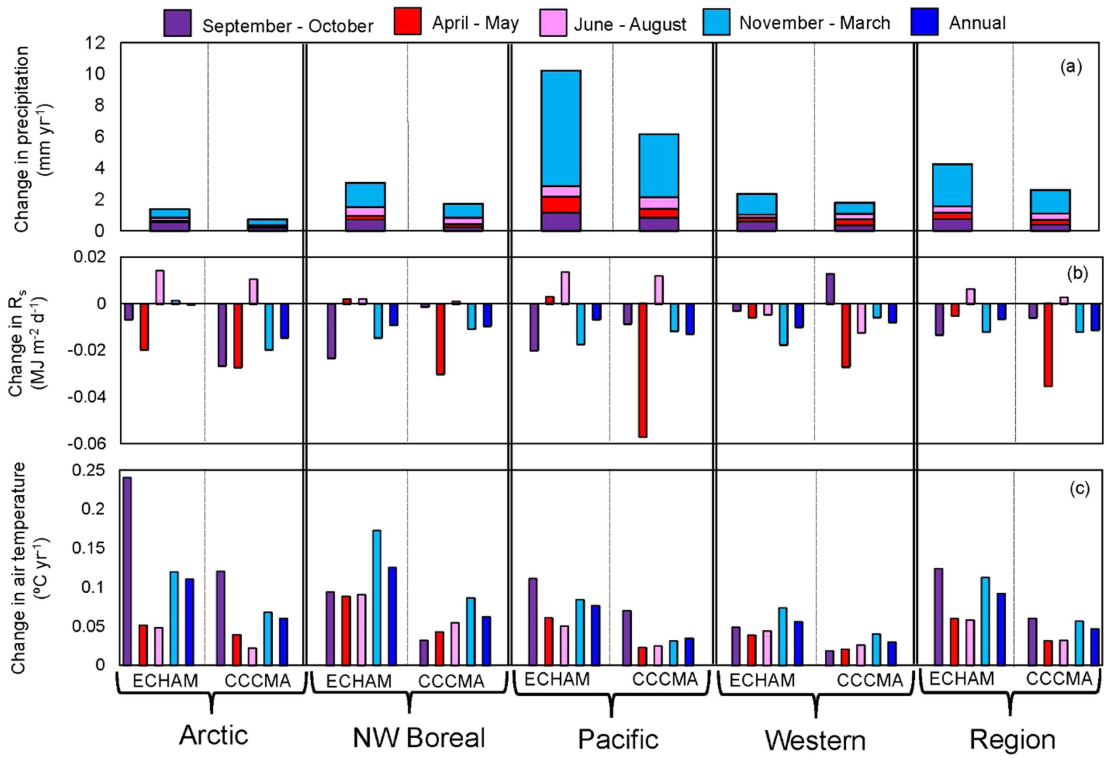

Figure 2. Trends in precipitation, incoming solar radiation, and air temperature across the four Landscape Conservation Cooperatives (Arctic, Northwest Boreal, Northern Pacific, Western Alaska) and regionally, during 2009–2100 based on the outputs from two general circulation models (ECHAM and CCCMA) and one scenario (A1B). Trends are based on the slopes of least-squares linear regression. Under the ECHAM scenario, the following trends are significant at $p < 0.0001$: precipitation in the fall in the Arctic LCC, incoming solar radiation in the Northwest Boreal LCC, air temperature in the winter in Arctic LCC, air temperature across all seasons in the Northwest Boreal and Western Alaska LCCs, and air temperature in the summer in the Pacific LCC. Under the CCCMA scenario, precipitation, incoming solar radiation, and air temperature in the winter in the Arctic LCC were the only trends significant at $p < 0.0001$.

ALFRESCO and DOS-TEM, the vegetation transitions and snow cover are summarized annually across each LCC prior to computing the decadal atmospheric heating feedbacks. Atmospheric heating feedbacks from each LCC are then area weighted by the proportion of the LCC to the total region such that the total regional feedback is the sum of the feedbacks from each LCC.

Results

Climate and snow cover

Across all regions, both GCMs showed trends towards warmer and wetter conditions between 2010 and 2099, although these increases in temperature and precipitation were consistently greater in the ECHAM scenario than the CCCMA scenario (figure 2). The Western Alaska LCC showed the smallest increases in temperature. The Arctic LCC showed the smallest increases in the amount of precipitation in both the ECHAM and CCCMA scenarios, although as a percentage this increase in precipitation could be as large as 70% more precipitation in the future between November and March compared to the historical record during these same months. Increases in precipitation were generally greatest during the cold season from November to March, followed by the fall shoulder season from September to October (figure 2(a)). The fall shoulder season generally showed the greatest warming across each of the four LCCs, followed by the cold season, from November to March (figure 2(c)). There was a general trend towards a decrease in incoming shortwave radiation across both models (figure 2(b)).

These differences in the amount of increase in temperature and precipitation across the two models resulted in differences in changes in the timing of snowmelt, snow return, and the duration of the snow season from 2010 to 2099 (figure 3). The snowmelt anomalies were greatest in the Western Alaska and North Pacific LCCs for the ECHAM scenario (figures 3(c) and (d)). In the Northwest Boreal LCC, the CCCMA scenario generally showed a later snowmelt anomaly from 2010 to 2099 (figure 3(b)). There was a greater change in the timing of snow return anomaly (figures (e)–(h)) compared to the change in the timing of snowmelt, with the change in snow return being smallest for the Northwest Boreal LCC under both the CCCMA and ECHAM scenarios (figure 3(f)). Overall, the change in the duration of the snow season was greatest in the Western Alaska LCC under the ECHAM scenario (an anomaly of 66 days shorter in the last decade, 2090–2099 compared to the

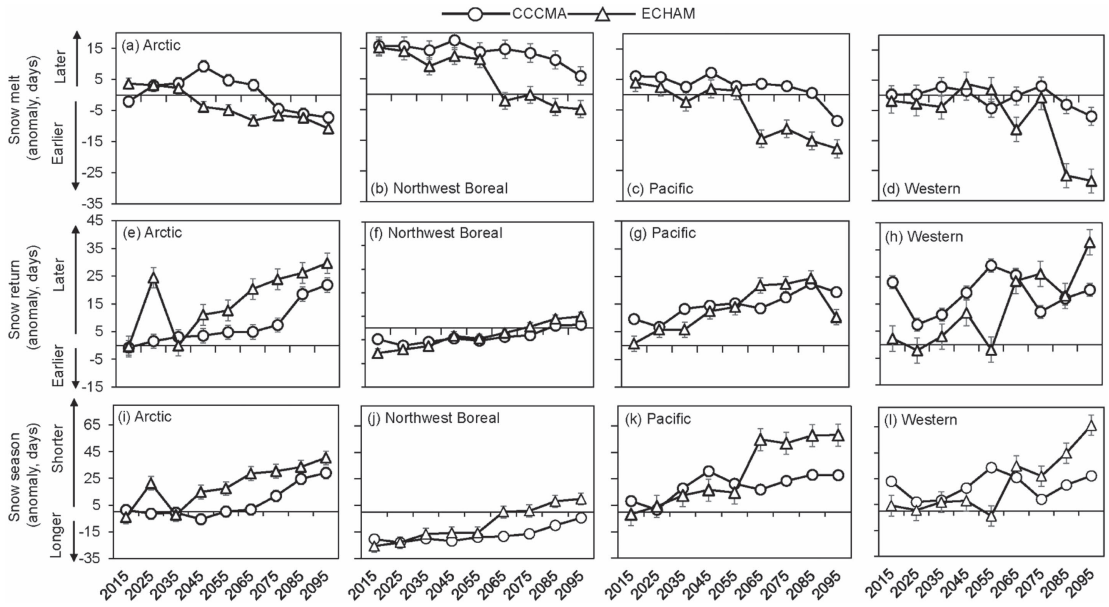

Figure 3. Anomalies of snow melt, snow return, and the duration for the snow season by decade between 2010 and 2099. Anomalies are calculated based on mean date of snow melt, snow return, and total snow cover duration from 1980 to 2009. For snowmelt, a positive anomaly indicates a later day of snow melt and a negative anomaly an earlier day of snowmelt. For snow return and the duration of the snow season, a positive anomaly indicates a later day of snow return or shorter snow cover duration, while a negative anomaly indicates an earlier snow return or longer snow cover duration.

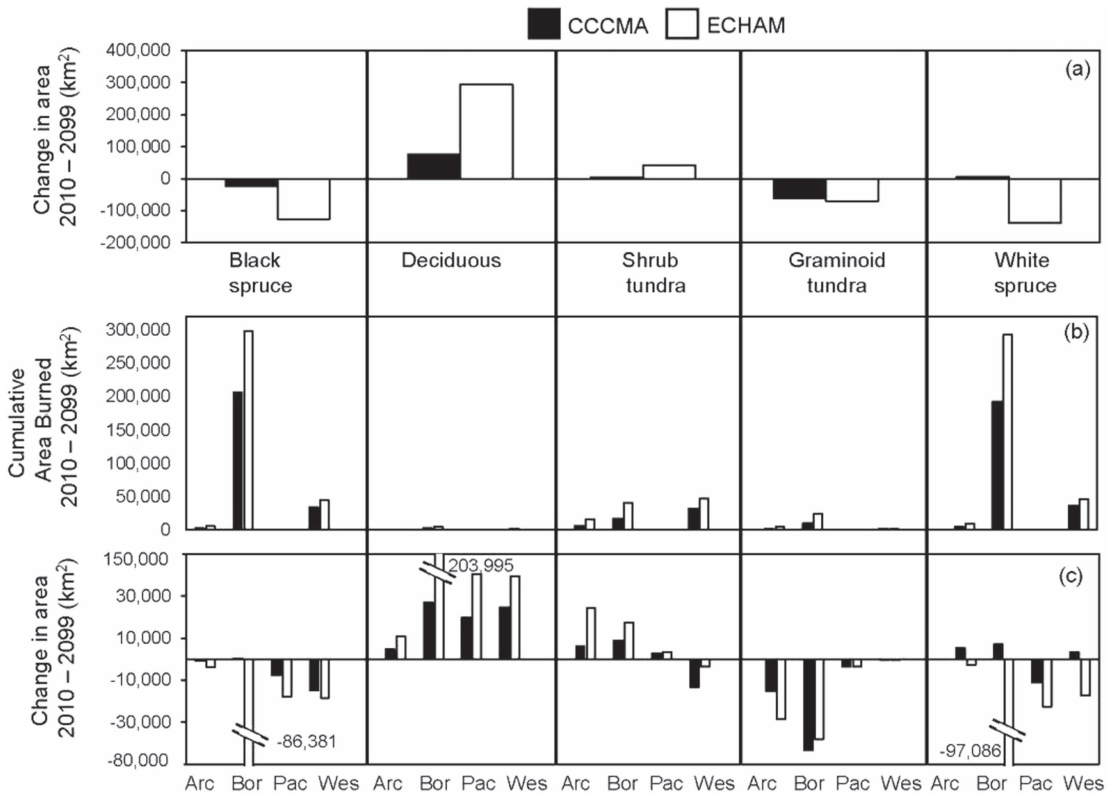

Figure 4. Changes in vegetation (km^2) (a), (c) and cumulative area burned (b) from 2010 to 2099 for the CCCMA and ECHAM scenarios. In (a), the overall change between the first decade (2010–2019) and last decade (2090–2099) in a vegetation type is shown, including changes due to shrubification, fire, treeline advance, and drought stress. In (b), the cumulative amount of each vegetation type that burned over the years 2010–2099 is depicted. Panel (c) depicts the overall change in a vegetation regionally, across all four LCCs. 'Arc' = Arctic LCC, 'Bor' = Northwestern Boreal LCC, 'Pac' = Pacific LCC, 'Wes' = Western Alaska LCC.

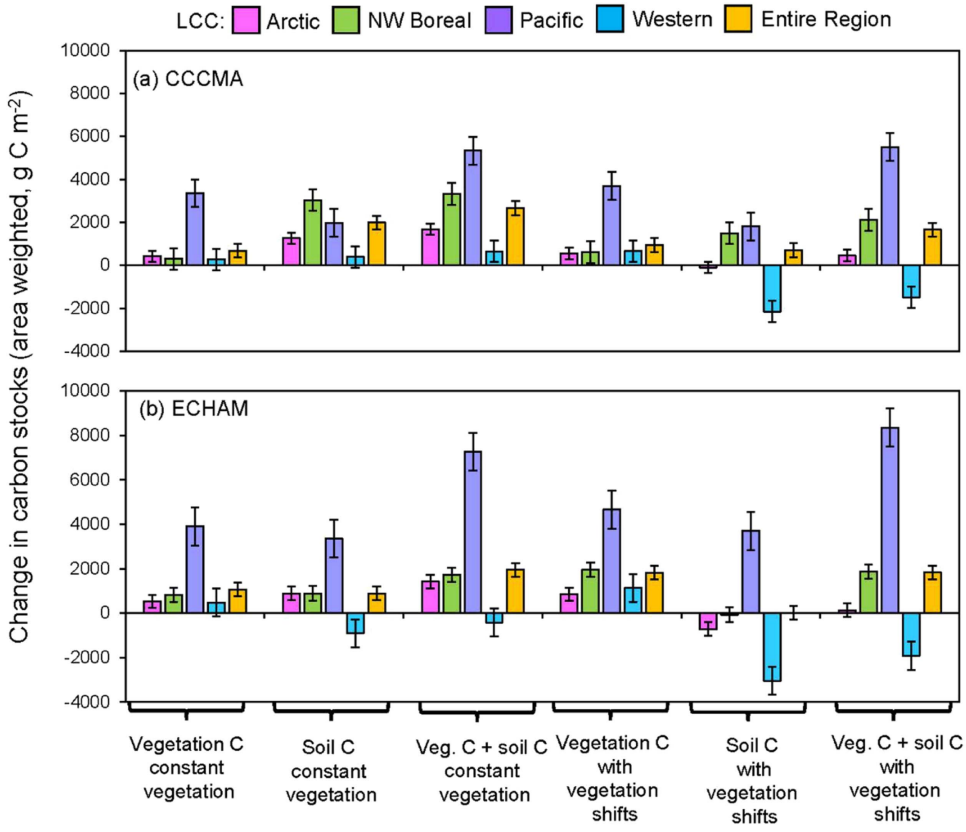

Figure 5. The overall changes in carbon stocks (g C m^{-2}), including vegetation and soil C between the first decade (2010–2019) and last decade (2090–2099) of the period of analysis for the CCCMA scenario (a) and ECHAM scenario (b). The C stocks by LCC are weighted by the proportion of each vegetation type in a given LCC, with vegetation types remaining constant to their proportions of each in the first decade ('constant vegetation') and with vegetation types shifting as modeled in ALFRESCO ('with vegetation shifts') between 2010 and 2099. The regional changes ('Entire Region') are weighted by the proportion of the vegetation type in each LCC and by the proportion of each LCC as a part of the total study region. Changes in vegetation and soil C by vegetation type for the CCCMA and ECHAM scenarios and LCC are provided in supplementary appendix 2.

mean snow duration from 1980 to 2009; figure 3(l)), with little change in the Northwest Boreal LCC under both the ECHAM and CCCMA scenarios (figure 3(j)).

Vegetation dynamics

Across the region between 2010 and 2099, there was a shift towards a decrease in later successional (⩾59 yrs) black and white spruce forests, and corresponding increases in early and mid-successional deciduous forests (0 to 59 yrs; figure 4(a); supplementary appendix 1; figures 1–3). No change was projected in land cover for maritime coastal temperate forest, barren lichen-moss (heath) tundra, or wetland tundra due to the static nature by which ALFRESCO treats these ecosystem types. Consequently, the projected land cover changes were smaller in the North Pacific LCC compared to the other LCCs since the dominant vegetation type in the North Pacific LCC is maritime coastal temperate forest. The decreases in the black and white spruce forests were due to both drought stress and burning. Early, and eventually, mid-successional deciduous forests generally replaced the black and white spruce forests. The loss of graminoid tundra was due to treeline advance, fire, and shrubification. Below, we further describe these vegetation dynamics.

In the Northwest Boreal LCC, there were similar losses of black and white spruce forest due to fire between the two scenarios (figure 4(b)). However, there was a much larger overall loss of black and white spruce forest in the ECHAM scenario compared to the CCCMA scenario (figure 4(c)), indicating that much of the boreal forest that burned in the CCCMA scenario eventually self-replaced by black or white spruce forest, while the forests in the ECHAM scenario burned more frequently and remained young deciduous forest. Although there was almost no fire in the Pacific LCC (figure 4(b)), there were shifts in vegetation due to natural successional processes, resulting in a decrease in black and white spruce forests and an overall increase in deciduous forests across both the CCCMA and ECHAM scenarios (figure 4(c)).

Across the Arctic, Northwest Boreal, and Western Alaska LCC, the shrub tundra was prone to fire, with greatest burn area in the Northwest Boreal and Western Alaska LCC under the ECHAM scenario (figure 4(b)). However, due to shrubification, these losses in shrub tundra from fire were alleviated in the

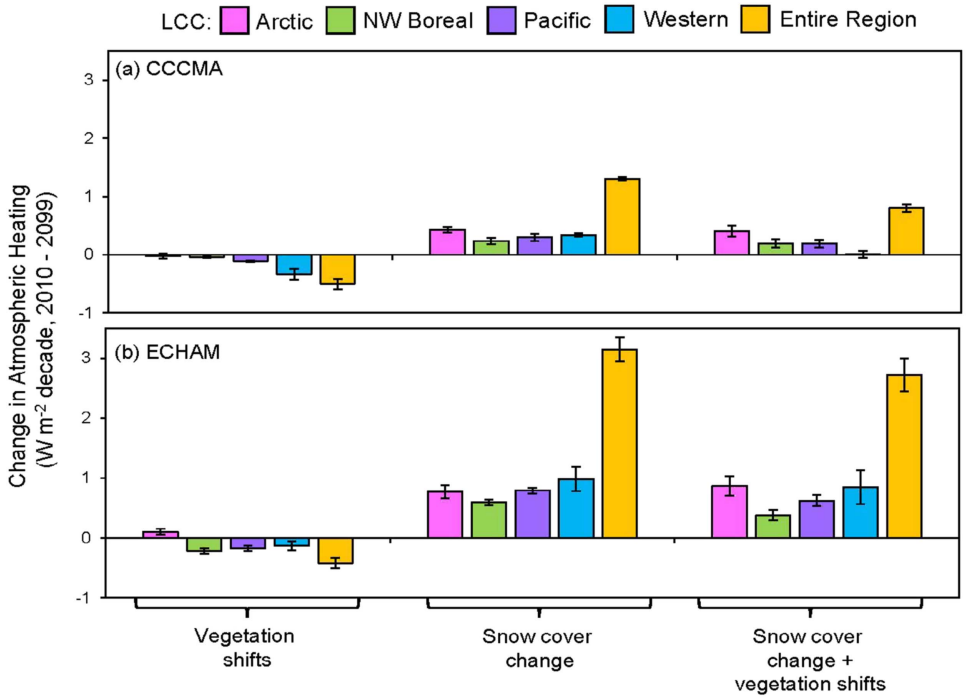

Figure 6. Changes in atmospheric heating (2010–2099, W m^{-2} $decade^{-1}$) due to biogeophysical factors (changes in vegetation cover and the snow season duration) for the CCCMA scenario (a) and ECHAM scenario (b). The regional changes ('Entire Region') are weighted by the proportion of the vegetation type in each LCC and by the proportion of each LCC as a part of the total study region.

Arctic and Northwest Boreal LCCs in both the ECHAM and CCCMA scenarios (figure 4(c)), resulting in an overall increase in the area of shrub tundra. This was not the case in the Western Alaska LCC, where the amount of shrubification was less than area of shrub tundra that burned under both the CCCMA and ECHAM scenarios, resulting in an overall loss of shrub tundra.

There were also losses in graminoid tundra across all scenarios due to fire, shrubification and treeline advance, with treeline advance, and the corresponding replacement of graminoid tundra with white spruce forest, accounting for the most of the loss. Regionally, this replacement totaled approximately 31 300 km^2 under the ECHAM scenario and 54 100 km^2 under the CCCMA scenario. The Northwest Boreal LCC comprised the greatest area where graminoid tundra either burned (figure 4(b)) or was lost due to treeline advance. Here, treeline advance accounted for a loss of approximately 22 000 km^2 for the ECHAM scenario and 35 000 km^2 for the CCCMA scenario in this LCC.

Vegetation and soil carbon

From 2010 to 2099, vegetation carbon pools increased (figure 5; supplementary appendix 2), even while the area covered by a given vegetation type may have decreased or remained static. There were two exceptions, both in the CCCMA scenario: a slight decrease in the Arctic LCC deciduous forests (−54 g C m^{-2}) and in the black spruce forests of the Western Alaska LCC (−68 g C m^{-2}). Those vegetation types that remained static in cover, barren lichen-moss (heath) tundra, wetland tundra, and coastal temperate forests, all showed increases in vegetation C (supplementary appendix 2). Out of all the vegetation types, the coastal temperate forests in the Pacific LCC showed the greatest increases in vegetation C, by +10 282 g C m^{-2} in the CCCMA scenario and by +11 746 g C m^{-2} in the ECHAM scenario, from 2010 to 2099.

Regionally, soil C also increased from 2010 to 2099, although some vegetation types showed overall decreases in soil C. This included both the CCCMA and ECHAM scenarios for the shrub and heath tundra in the Arctic LCC, the black spruce forests in the Northwest Boreal LCC under the ECHAM scenario, and the deciduous forests in the Pacific LCC under the ECHAM scenario. Notably, in the ECHAM scenario, the Western Alaska LCC showed decreases in soil C across all vegetation types, except for the graminoid tundra and white spruce forests, and in the CCCMA scenario, soil C in this LCC decreased in the black spruce forests and heath tundra.

Regionally, from 2010 to 2099, when considering shifts across the vegetation types, the total change in vegetation and soil C was similar between the two scenarios: +1654 g C m^{-2} for the CCCMA scenario and +1829 g C m^{-2} for the ECHAM scenario. If the vegetation remained constant, then the estimates differed by 720 g C m^{-2}, with a change of +2674 g C m^{-2} in the CCCMA scenario and +1954 g C m^{-2} in the ECHAM scenario (figure 5).

Atmospheric heating and feedbacks to climate

Vegetation shifts resulted in a regional negative feedback to climate of −0.42 to 0.52 W m^{-2} $decade^{-1}$ for the ECHAM and CCCMA scenarios, respectively (figure 6). The largest negative feedback occurred in the Western Alaska LCC under the CCCMA scenario (−0.34 W m^{-2} $decade^{-1}$; figure 6(a)), and was due to the negative feedback associated with the decrease in shrub tundra following fire, and replacement by graminoid tundra. This negative feedback was large enough to cancel the positive feedback due to changes in snow cover in the Western Alaska LCC under the CCCMA scenario. The second largest negative feedback occurred under the ECHAM scenario in the Northwest Boreal LCC (−0.22 W m^{-2} $decade^{-1}$; figure 6(b)). This coincided with the shift from white and black spruce forests to deciduous forests under an intensified fire regime. The only scenario where vegetation shifts resulted in a positive climate feedback was in the Arctic LCC under the ECHAM scenario. This small positive feedback (0.10 W m^{-2} $decade^{-1}$; figure 6(b)) was due to both an advancement of treeline and shrubification, and a fire regime of low intensity.

There was an overall positive feedback to atmospheric heating when changes in snow cover were considered in concert with changes in vegetation (figure 6). This positive feedback was larger in the ECHAM scenario across all LCCs (2.7 W m^{-2} $decade^{-1}$ over all LCCs) compared to the CCCMA scenario (0.76 W m^{-2} $decade^{-1}$ over all LCCs) due to the greater reduction in the length of the snow season in the ECHAM scenario (figure 3). The positive feedback was greatest in the Arctic and Western Alaska LCCs under the ECHAM scenario (~0.85 W m^{-2} $decade^{-1}$ from each LCC; figure 6(b)).

While we did not explicitly estimate the biogeochemical feedbacks due to changes in carbon storage in the vegetation and soils, the increases in C storage indicated that there would be an overall negative feedback to climate in all LCCs except the Western Alaska LCC, where losses in soil C were larger than increases in vegetation C (figure 5). While the biogeophysical feedbacks were small in the Western Alaska LCC (figure 6), large increases in vegetation and soil C in both the CCCMA and ECHAM scenarios by the maritime coastal temperate forests in the North Pacific LCC (figure 5) indicated that this region may be important to consider in terms of climate feedbacks related to changes in C cycling.

Discussion

Overview

Across Alaska and northwest Canada, we simulated changes in vegetation composition, snow cover, and vegetation and soil C stocks under one emissions scenario (A1B) and the climate outputs from two general circulation models, CCCMA and ECHAM. Our simulations occurred at a 1 km^2 spatial scale, which is an unprecedented amount of detail for this region. We found that changes in snow cover duration, including both the timing of snowmelt in the spring and snow return in the fall, provided the dominant positive biogeophysical feedback to climate across all LCCs, while changes in vegetation composition generally resulted in negative biogeophysical feedbacks to climate. We expect that there would be a negative biogeochemical feedback to climate since vegetation C increased across all LCCs, and soil C increased across all LCCs except the Arctic LCC under the ECHAM scenario and the Western Alaska LCC under both scenarios. Although other studies have simulated some of these types of feedbacks in high latitudes (e.g., Groisman *et al* 1994, Betts 2000, Randerson *et al* 2006, Loranty *et al* 2011, 2014, de Wit *et al* 2014), this study provides a comprehensive comparative approach across the ecoregions in Alaska and northwest Canada. Below, we discuss additional details related to these feedbacks and consider other forcing agents that may be important to consider in future studies.

Biogeophysical feedbacks due to changes in vegetation composition

Our results emphasize the importance of considering both tundra and boreal forest wildfire. In the tundra, it was particularly important to consider the burning of shrub tundra. Although studies have suggested that an increase in shrub tundra will act as a positive feedback to climate warming since these shrubs have a lower albedo and greater sensible heat flux than graminoid tundra, previous work has not considered these feedbacks in association with increased burning of shrub tundra (Sturm *et al* 2005, Euskirchen *et al* 2009b, Bonfils *et al* 2012, Zhang *et al* 2014). Here, we found that while significant amounts of shrub tundra burned in the Arctic, Boreal, and Western Alaska LCCs (figure 4(b)), in the Arctic and Boreal LCCs, there were also increases in the amount of shrub tundra (figure 4(a)) large enough to counteract the greater albedo associated with the burned shrub tundra. In the Western Alaska LCC, there was an overall decrease in shrub tundra, resulting in a negative feedback to climate warming in the CCCMA scenario (figure 6). It is also important to note that shrub height, relative to snow cover thickness, has a key influence over feedbacks to climate, where research shows that shrubs of 0.5 m height having a significantly smaller influence on atmospheric heating than shrubs of 2 m in height (Bonfils *et al* 2012). Here, our parameterizations of the radiation and energy fluxes for shrub tundra (table 1) were based on a site with shrubs of ~1 m in height, with shrubs partially exposed all winter. Thus, the positive biogeophysical climate feedbacks associated with shrub expansion would likely be less for the shorter shrubs $\leqslant$0.5 m in height, but greater than the taller shrubs $>$1 m in height.

Wildfire was also important in the Northwest Boreal LCC, with both the CCCMA and ECHAM scenarios indicating large losses of black and white spruce forests that were replaced by young, early successional deciduous forests. This loss of black and white spruce forest was greater in the warmer ECHAM scenario compared to the CCCMA scenario (figure 4(b)). These results support the concept that large expanses of black and white spruce forests in this region may be converted to grasslands or aspen/birch parklands in the coming century under warmer temperatures and an intensified fire regime (Chapin *et al* 2004, Johnstone *et al* 2010, Kasischke 2010). The grasslands and deciduous trees (aspen, birch) that establish following fire have a summer and winter albedo that is greater than the coniferous ecosystems (Amiro *et al* 2006, Liu and Randerson 2008; table 1), thereby resulting in a negative feedback to climate (Beck *et al* 2011, Rogers *et al* 2013).

Although fire proved a critical component of this analysis, the biogeophysical climate feedback due to the advance in treeline was negligible. The Northwest Boreal LCC had the greatest increase in the advancement of treeline, but the estimate of this positive feedback was miniscule ($\ll$1 W m^{-2} for the 90 years from 2010 to 2099). This differs from some other studies in other regions that have found stronger localized positive feedbacks to climate warming associated with changes in treeline (e.g., Pearson *et al* 2013, deWit *et al* 2014), and may be due to differences in forest species or faster estimated rates of treeline advance. It is also important to note that in our study area, the Brooks Range provides a natural barrier to treeline expansion (Rupp *et al* 2001).

Snow cover

It is now well known that changes in snow cover, particularly in spring, can have a strong impact on regional energy budgets due to the considerable amount of incoming solar energy reaching the snow surface (Groisman *et al* 1994, Déry and Brown 2007, Euskirchen *et al* 2007). We previously estimated that a pan-Arctic reduction in snow cover of 0.22 day yr^{-1} during the 1970–2000 period of warming contributed an additional 0.8 W m^{-2} per decade of energy (Euskirchen *et al* 2007), a result which is similar to that seen here in the CCCMA scenario (figure 6(a)) for this study region in Alaska and northwest Canada. When comparing climate feedbacks associated with changes in shrub tundra growth to changes in snow cover in arctic Alaska (Euskirchen *et al* 2009b), we found that greater aboveground biomass from increased shrub NPP produced a decrease in summer albedo, greater regional heat absorption (0.34 $\pm$ 0.23 W m^{-2} decade^{-1}), and a net positive feedback to climate warming. However, this positive feedback was much smaller than the positive feedback due to a shorter snow season (3.3 $\pm$ 1.24 W m^{-2} decade^{-1}; Euskirchen *et al* 2009b).

Carbon storage

Our simulations with TEM indicated overall increases in carbon storage in the vegetation and soils across the study region, which would result in an estimated negative feedback to climate. Previous simulations with TEM have shown that increases in C storage are associated with the fertilization effect of a rising CO_2 concentration (e.g., Hayes *et al* 2011). Thus, with greater productivity under higher CO_2 concentrations, C inputs from litterfall increase, resulting in soil C storage. Historical estimates of simulated soil C stocks and heterotrophic respiration in TEM fall within the range of simulations with other biogeochemistry models across Alaska (Fischer *et al* 2014). One way to quantify the biogeochemical feedbacks to climate from carbon storage is to employ a fully coupled model of both biogeochemistry and climate that includes the high-level of detail in the arctic and boreal vegetation dynamics we incorporate here, while other methodology can also be implemented (e.g., Frolking *et al* 2006, Ward *et al* 2012, Bright *et al* 2016). It is important to recognize that biogeochemical feedbacks are a global phenomenon, while energy budget feedbacks are predominately local to regional.

The Western Alaska LCC showed loss of soil C, but there is greater uncertainty in this remote region due to a lack of observational data pertaining to climate, vegetation, soils, and disturbance. In future work in the four LCCs considered here, it may be also important to examine the losses of soil C associated directly with regional thawing permafrost and an intensified fire regime. Furthermore, it is important to consider differences in the drier uplands versus the wet lowlands. Simulations with TEM show that the 12% of the study region that is considered lowlands are sources of C, while the uplands are sinks of C (Zhu and McGuire 2016, chapters 6 and 7). We did not include changes in methane (CH_4) consumption in our estimate of feedbacks to climate. However, the wetlands in our study region are estimated as increasing sources of CH_4, and were the primary reason that the wetlands in the study region were estimated as sources of C (Zhu and McGuire 2016, chapter 7). Consequently, given the smaller proportion of lowlands than uplands, in this present regional assessment, the area remained a C sink, but an expansion of wetlands may result in a greater area that acts as a C source.

Since the version of TEM used here has been developed specifically and optimized for this region, other biogeochemical models with less specific development for our study area may show different results. For example, recent work shows large differences among land surface and biogeochemical models simulated in Arctic Alaska (McGuire *et al* 2012, Fisher *et al* 2014). Much uncertainty across models might be associated with differences in the representation of permafrost and to winter respiration (Belshe *et al* 2013).

Other forcing agents

Other forcing agents that we did not take into account, but which are present in our study area, include thermokarst formation, insect outbreaks, and shifts in the maritime coastal temperate forests. Increases in thermokarst formation (ground subsidence following permafrost thaw) may result in either a negative or positive feedback to climate. In boreal regions, areas that were previously forested, typically by spruce, may become bogs or fens (Jorgenson *et al* 2001), with a greater albedo and act as a negative biogeophysical feedback to climate. For example, data gathered from a thermokarst collapse scar bog (50 years old) and a moderate rich fen both show year round higher values of albedo and less atmospheric heating compared to spruce and deciduous forests (table 1). As a biogeochemical feedback to climate these thermokarst bogs and fens may sequester either more or less carbon (O'Donnell *et al* 2012, Jones *et al* 2013, Euskirchen *et al* 2014), making their net effect unknown. In arctic regions, typical thermokarst landforms include thermokarst lakes, collapsed pingos, sinkholes, and pits. A key question, both in arctic tundra and boreal forests, is if the number of newly formed thermokarst features would cover a large enough area to induce a significant change in land surface albedo and energy fluxes. Again, a related question is how the creation of these landforms alters the overall carbon storage capacity of the region (Walter Anthony *et al* 2014, Abbott and Jones 2015), and how this impacts the overall feedback to climate.

Across the forested portions our study area, insect damage can play an important role in tree mortality (FS-R10-FHP 2015). Under warming temperatures in recent decades, a reduction of the beetle life cycle from 2 years to 1 year has in part led to severe spruce beetle outbreaks, with widespread white spruce mortality (Werner *et al* 2006). Increased disturbance from insect outbreaks will also shift the forest to a younger age classes (Boucher and Mead 2006, Kurz *et al* 2008) increasing the surface albedo, possibly leading to a negative feedback on atmospheric heating. However, this negative feedback could be counterbalanced by reduced carbon storage capacity in these mature forests with insect outbreaks (Kurz *et al* 2008).

In future studies that include the North Pacific LCC, it may also be important to include shifts in the maritime coastal temperate forests, which have experienced documented mortality related to climate change (Hennon *et al* 2012). For example, mortality in yellow-cedar in this region has been related to earlier snowmelt and later freeze-up, where over 200 000 ha of forests have died in the past 100 years (Hennon *et al* 2006). Moreover, these forests can attract and hold cloud cover, which reflect heat and sunlight (Lawford *et al* 1996). This potentially strong negative feedback to climate, combined with these forest's carbon storage, are important factors to consider in light of net feedbacks to climate.

Conclusion

A continuing challenge in global change studies is to determine how land surface changes may impact atmospheric heating. Here, we show that even when accounting for a greater number of possible positive feedbacks to climate due to shifts in vegetation than previous studies, including both boreal and tundra fire, an advance of treeline, and increases in the distribution of shrub tundra, changes in snow cover still provided the dominant biogeophysical, land surface positive feedback to atmospheric heating. This positive feedback was partially moderated by an increase in area burned in spruce forests and shrub tundra. It is important to continue to detect changes in vegetation and snow cover, and to combine our knowledge of terrestrial response with that in aquatic environments, including land surface changes caused by a reduction of sea ice, to reach a better understanding of how northern high-latitude ecosystems will influence the climate system.

Acknowledgments

This research was primarily supported by funding from U.S. Geological Survey Alaska Climate Science Center; the Arctic, Northwest Boreal, and Western Alaska Landscape Conservation Cooperatives; and the U.S. Geological Survey Alaska Land Carbon Project. Support was also provided by National Science Foundation through the Bonanza Creek Long Term Ecological Research Program, the Department of Defense's Strategic Environmental Research and Development Program (Project RC-2110), the Department of Energy through the Next-Generation Ecosystem Experiments (NGEE-Arctic), and the EPSCoR Program of the National Science Foundation. Any use of trade, firm, or product names is for descriptive purposes only and does not imply endorsement by the U.S. Government. We thank two anonymous reviews whose comments helped to improve the manuscript.

References

Abbott B W and Jones J B 2015 Permafrost collapse alters soil carbon stocks, respiration, CH_4, and N_2O in upland tundra *Glob. Change Biol.* **21** 4570–87

Allen R G, Pereira L S, Raes D and Smith M 1998 Crop evapotranspiration—guidelines for computing crop water requirements *FAO Irrigation and Drainage Paper. No. 56* Water Resources, Development and Management Service, Food and Agriculture Organization of the U.N., Rome

Amiro B D *et al* 2006 The effect of post-fire stand age on the boreal forest energy balance *Agric. For. Meteorol.* **140** 41–50

Balshi M S, McGuire A D, Duffy P, Flannigan M, Kicklighter D W and Melillo J 2009 Vulnerability of carbon storage in North American boreal forests to wildfires during the 21st century *Glob. Change Biol.* **15** 1491–510

Barber V A, Juday G P and Finney B P 2000 Reduced growth of Alaskan white spruce in the twentieth century from temperature-induced drought stress *Nature* **405** 668–73

Beck P S A, Goetz S J, Mack M C, Alexander H D, Jin Y, Randerson J T and Loranty M M 2011 The impacts and implications of an intensifying fire regime on Alaskan boreal forest composition and albedo *Glob. Change Biol.* **17** 2853–66
Belshe E F, Schuur E A G and Bolker B M 2013 Tundra ecosystems observed to be CO_2 sources due to differential amplification of the carbon cycle *Ecol. Lett.* **16** 1307–15
Betts A K and Ball J H 1997 Albedo over the boreal forest *J. Geophys. Res.* **102** 28901–9
Betts R A 2000 Offset of the potential carbon sink from boreal forestation by decreases in surface albedo *Nature* **408** 187–90
Binkley D 1982 Nitrogen fixation and net primary production in a young Sitka alder stand *Can. J. For. Res.* **12** 281–4
Bonan G B 2008 Forests and climate change: forcings, feedbacks, and the climate benefits of forests *Science* **320** 1444–9
Bonfils C J W, Phillips T J, Lawrence D M, Cameron-Smith P, Riley W J and Subin Z M 2012 On the influence of shrub height and expansion on northern high latitude climate *Environ. Res. Lett.* **7** 015503
Boucher T V and Mead B R 2006 Vegetation change and forest regeneration on the Kenai Peninsula, Alaska, following a spruce beetle outbreak, 1987–2000 *For. Ecol. Manage.* **227** 233–46
Bright R M, Bogren W, Bernier P and Astrup R 2016 Carbon-equivalent metrics for albedo changes in land management contexts: relevance of the time dimension *Ecol. Appl.* **26** 1868–80
Brownlee A H, Sullivan P F, Csank A Z, Sveinbjörnnson B and Ellison S B 2016 Drought-induced stomatal closure probably cannot explain divergent white spruce growth in the Brooks Range, Alaska USA *Ecology* **97** 145–59
Calef M P, Varvak A, McGuire A D, Chapin F S III and Reinhold K B 2015 Recent changes in annual area burned in interior Alaska: the impact of fire management *Earth Interact.* **19** 1–17
Chapin F S III, Callaghan T V, Bergeron Y, Fukuda M, Johnstone J F, Juday G and Zimov S A 2004 Global change and the boreal forest: thresholds, shifting states, or gradual change *Ambio* **33** 361–5
Chapin F S III *et al* 2000 Arctic and boreal ecosystems of western North America as components of the climate system *Glob. Change Biol.* **6** 211–23
Chapin F S III *et al* 2005 Role of land surface changes in arctic summer warming *Science* **310** 657–60
Callaghan T V *et al* 2011 The changing face of arctic snow cover: a synthesis of observed and projected changes *Ambio* **40** 17–31
Clein J S, McGuire A D, Zhang X, Kicklighter D W, Melillo J M, Wofsy S C, Jarvis P G and Massheder J M 2002 Historical and projected carbon balance of mature black spruce ecosystems across North America: the role of carbon–nitrogen interactions *Plant Soil* **242** 15–32
D'Amore D V, Fellman J B, Edwards R T, Hood E and Ping C-L 2012 Hydropedology of the North American coastal temperate rainforest, *Hydropedology: Synergystic Integration of Soil Science and Hydrology* ed H Lin (Waltham, Mass.: Academic) pp 351–80
Daly C, Halbleib M, Smith J I, Gibson W P, Doggett M K, Taylor G H, Curtis J and Pasteris P P 2008 Physiographically sensitive mapping of climatological temperature and precipitation across the conterminous United States International *J. Climatol.* **28** 2031–64
de Wit H A, Bryn A, Hofgaard A, Karstensen J, Kvalevåg M M and Peters G P 2014 Climate warming feedback from mountain birch forest expansion: reduced albedo dominates carbon uptake *Glob. Change Biol.* **7** 2344–55
Déry S J and Brown R D 2007 Recent northern hemisphere snow cover extent trends and implications for the snow-albedo feedback *Geophys. Res. Lett.* **34** L22504
Duffy P A, Walsh J E, Graham J M, Mann D H and Rupp T S 2005 Impacts of large-scale atmospheric-ocean variability on Alaskan fire season severity *Ecol. Appl.* **15** 1317–30
Dye D G 2002 Variability and trends in the annual snow-cover cycle in Northern Hemisphere land areas, 1972–2000 *Hydrol. Process.* **16** 3065–77
Eugster W *et al* 2000 Land-atmosphere energy exchange in Arctic tundra and boreal forest: available data and feedbacks to climate *Glob. Change Biol.* **6** 84–115
Euskirchen E S *et al* 2006 Importance of recent shifts in soil thermal dynamics on growing season length, productivity, and carbon sequestration in terrestrial high-latitude ecosystems *Glob. Change Biol.* **12** 731–50
Euskirchen E S, Bret-Harte M S, Scott G J, Edgar C and Shaver G R 2012 Seasonal patterns of carbon dioxide and water fluxes in three representative tundra ecosystems in northern Alaska *Ecosphere* **3** 1–19
Euskirchen E S, Edgar C, Turetsky M R, Waldrop M P and Harden J W 2014 Differential response of carbon fluxes to climate in three peatland ecosystems that vary in the presence and stability of permafrost *J. Geophys. Res.—Biogeosci.* **119** 1576–95
Euskirchen E S, McGuire A D and Chapin F S III 2007 Energy feedbacks of northern high-latitude ecosystems to the climate system due to reduced snow cover during 20th century warming *Glob. Change Biol.* **13** 2425–38
Euskirchen E S, McGuire A D, Chapin F S III and Rupp T S 2010 The changing effects of Alaska boreal forests on the climate system *Can. J. For. Res.* **40** 1336–46
Euskirchen E S, McGuire A D, Chapin F S III, Yi S and Thomspon C C 2009b Changes in vegetation in northern Alaska under scenarios of climate change 2003–2100: implications for climate feedbacks *Ecol. Appl.* **19** 1022–43
Euskirchen E S, McGuire A D, Rupp T S, Chapin F S III and Walsh J E 2009a Projected changes in atmospheric heating due to changes in fire disturbance and the snow season in the western Arctic, 2003–2100 *J. Geophys. Res.—Biogeosciences* **114** 15
Fisher J B *et al* 2014 Carbon cycle uncertainty in the Alaskan Arctic *Biogeosciences* **11** 4271–88
Flato G M 2005 The third generation coupled global climate model (CGCM3) (and included links to the description of the AGCM3 atmospheric model): Canadian Centre for Climate Modelling and Analysis (http://ec.gc.ca/ccmac-cccma/default.asp?lang=En&n=1299529F-1)
Frolking S, Roulet N and Fuglestvedt J 2006 How northern peatlands influences the Earths radiative budget: Sustained methane emission versus carbon sequestration *J. Geophys. Res.* **111** G01008
FS-R10-FHP 2015 *Forest Health Conditions in Alaska 2014* (Anchorage, Alaska: U.S. Forest Service, Alaska Region) 88pp Publication R10-PR-36
Geiger R, Aron R A and Todhunder P 2009 *The Climate Near the Ground* 7th edn (New York: Rowan and Littlefield) 623 pp
Genet H *et al* 2013 Modeling the effects of fire severity and climate warming on active layer thickness and soil carbon storage of black spruce forests across the landscape in interior Alaska *Environ. Res. Lett.* **8** 13
Gorham E 1991 Northern peatlands: role in the carbon cycle and probable response to climatic warming *Ecol. Appl.* **1** 182–95
Gough L, Moore J C, Shaver G R, Simpson R T and Johnson D R 2012 Above- and belowground responses of arctic tundra ecosystems to altered soil nutrients and mammalian herbivory *Ecology* **93** 1683–94
Groisman P Y, Karl T R and Knight R W 1994 Observed impact of snow cover on the heat balance and the rise of continental spring temperatures *Science* **263** 198–200
Gustine D D, Brinkman T J, Lindgren M A, Schmidt J I, Rupp T S and Adams L G 2014 Climate-driven effects of fire on winter habitat for caribou in the Alaskan-Yukon Arctic *PLoS One* **9** 11
Harris I, Jones P, Osborn T and Lister D 2014 Updated high-resolution grids of monthly climatic observations—the CRU TS3.10 dataset *Int. J. Climatol.* **34** 623–42
Hay L E, Wilby R L and Leavesley G H 2000 A comparison of delta change and downscaled GCM scenarios for three mountainous basins in the United States *J. Am. Water Resour. Assoc.* **36** 387–97

Hayes D J, McGuire A D, Kicklighter D W, Gurney K R, Burnside T J and Melillo J M 2011 Is the northern high-latitude land-based CO_2 sink weakening? *Glob. Biogeochem. Cycles* **25** GB3018

Hayhoe K A 2010 A standardized framework for evaluating the skill of regional climate downscaled techniques: Urbana-Champaign, Illinois *PhD Dissertation* University of Illinois 153 p

Hennon P, D'Amore D, Wittwer D, Johnson A, Schaberg P, Hawley G, Beier C, Sink S and Juday G 2006 Climate warming, reduced snow, and freezing injury could explain the demise of yellow-cedar in southeast Alaska, USA *World Resour. Rev.* **18** 427–50

Hennon P E, D'Amore D V, Schaberg P G, Wittwer D T and Shanley C S 2012 Shifting climate, altered niche, and a dynamic conservation strategy for yellow-cedar in the North Pacific coastal rainforest *BioScience* **62** 147–58

Hewitt R E, Bennett A P, Breen A L, Hollingsworth T N, Taylor D L, Chapin F S III and Rupp T S 2015 Getting to the root of the matter: landscape implications of plant–fungal interactions for tree migration in Alaska *Landscape Ecol.* **31** 895–911

Hobbie S E 1996 Temperature and plant species control over litter decomposition in Alaskan tundra *Ecol. Monogr.* **66** 503–22

Hu F S, Higuera P E, Duffy P, Chipman M L, Rocha A V, Young A M, Kelly R and Dietze M C 2015 Arctic tundra fires: natural variability and responses to climate change *Front. Ecol. Environ.* **7** 369–77

Hugelius G *et al* 2014 Estimated stocks of circumpolar permafrost carbon with quantified uncertainty ranges and identified data gaps *Biogeosciences* **11** 6573–93

Idso S B and Jackson R D 1969 Thermal radiation from the atmosphere *J. Geophys. Res.* **74** 5397–403

IPCC 2013 *Climate Change 2013: The Physical Science Basis. Contribution of Working Group I to the Fifth Assessment Report of the Intergovernmental Panel on Climate Change* ed T F Stocker *et al* (Cambridge: Cambridge University Press) 1535 pp (doi:10.1017/CBO9781107415324)

Johnson K D *et al* 2011 Soil carbon distribution in Alaska in relation to soil-forming factors *Geoderma* **167–168** 71–84

Johnstone J F, Hollingsworth T N, Chapin F S III and Mack M C 2010 Changes in fire regime break the legacy lock on successional trajectories in Alaskan boreal forest *Glob. Change Biol.* **16** 1281–95

Johnstone J F, Rupp T S, Olson M and Verbyla D 2011 Modeling impacts of fire severity on successional trajectories and future fire behavior in Alaskan boreal forests *Landscape Ecol.* **26** 487–500

Jones M C, Booth R K, Yu Z and Ferry P 2013 A 2200-year record of permafrost dynamics and carbon cycling in a collapse-scar bog, Interior Alaska *Ecosystems* **16** 1–19

Jorgenson M T, Racine C H, Walters J C and Osterkamp T E 2001 Permafrost degradation and ecological changes associated with a warming climate in central Alaska *Clim. Change* **48** 551–79

Kasischke E S 2010 Alaska's changing fire regime—implications for the vulnerability of its oreal forests *Can. J. For. Res.* **40** 1313–24

Kurz W A, Dymond C C, Stinson G, Rampley G J, Neilson E T, Carroll A L, Ebata T and Safranyik L 2008 Mountain pine beetle and forest carbon feedback to climate change *Nature* **452** 987–90

Lawford R G, Alaback P and Fuentes E 1996 High-latitude rainforests and associated ecosystem of the west coast of the Americas *Climate, Hydrology, Ecology, and Conservation* (New York: Springer) 413 pp

Lloyd A H 2005 Ecological histories from Alaskan tree line provide insight into future change *Ecology* **86** 1687–95

Liu H and Randerson J T 2008 Interannual variability of surface energy exchange depends on stand age in a boreal forest fire chronosequence *J. Geophys. Res.* **113** G01006

Loranty M M, Berner L T, Goetz S J, Jin Y and Randerson J T 2014 Vegetation controls on northern high latitude snow-albedo feedback: observations and CMIP5 model simulations *Glob. Change Biol.* **2** 594–606

Loranty M M, Goetz S J and Beck P S A 2011 Tundra vegetation effects on pan-Arctic albedo *Environ. Res. Lett.* **6** 024014

Lynch A H, Bonan G B, Chapin F S III and Wu W 1999 Impact of tundra ecosystems on the surface energy budget and climate of Alaska *J. Geophys. Res.* **104** 6647–60

McFadden J P and Chapin F S III 1998 Subgrid-scale variability in the surface energy balance of the arctic tundra *J. Geopys. Res.* **103** 28947–61

McFarlane N A, Boer G J, Blanchet J-P and Lazare M 1992 The Canadian Climate Centre second-generation general circulation model and its equilibrium climate *J. Clim.* **5** 1013–44

McGuire A D, Melillo J M, Joyce L A, Kicklighter D W, Grace A L, Moore B III and Vorosmarty C J 1992 Interactions between carbon and nitrogen dynamics in estimating net primary productivity for potential vegetation in North America *Glob. Biogeochem. Cycles* **6** 101–24

McGuire A D *et al* 2012 An assessment of the carbon balance of arctic tundra: comparisons among observations, process models, and atmospheric inversions *Biogeosciences* **9** 4543–94

Malone T, Liang J and Packee E C 2009 *General Technical Report* PNW-GTR-785 Cooperative Alaska Forest Inventory: U.S. Department of Agriculture, Forest Service, Pacific Northwest Research Station 42 p

Mack M C, Bret-Harte M S, Hollingsworth T N, Jandt R R, Schuur E A G, Shaver G R and Verbyla D L 2011 Carbon loss from an unprecedented Arctic tundra wildfire *Nature* **475** 489–92

Mann D H, Rupp T S, Olson M A and Duffy P A 2012 Is Alaska's boreal forest now crossing a major ecological threshold? *Arct. Antarct. Alp Res.* **44** 319–31

Millard M J *et al* 2012 A national geographic framework for guiding conservation on a landscape scale *J. Fish Wildl. Manage.* **3** 175–83

Mueller C W *et al* 2015 Large amounts of labile organic carbon in permafrost soils of Northern Alaska *Glob. Change Biol.* **7** 2804–17

Myers-Smith I H *et al* 2015 Climate sensitivity of shrub growth across the tundra biome *Nat. Clim. Change* **5** 887–91

Nakicenovic N and Swart R (ed) 2000 *IPCC [Intergovernmental Panel on Climate Change] Emissions Scenarios* (Cambridge: Cambridge University Press) 570 p

Natali S M, Schuur E A G and Rubin R L 2012 Increased plant productivity in Alaskan tundra as a result of experimental warming of soil and permafrost *J. Ecol.* **100** 488–98

O'Donnell J A, Jorgenson M T, Harden J W, McGuire A D, Kanevskiy M Z and Wickland K P 2012 The effects of permafrost thaw on soil hydrologic, thermal and carbon dynamics in an Alaskan peatland *Ecosystems* **15** 213–29

Parkinson C L and Washington W M 1979 A large-scale numerical model of sea ice *J. Geophys. Res.* **84** 311–37

Payette S 1992 Fire as a controlling process in North American boreal forest *A Systems Analysis of the Global Boreal Forest* ed H H Shugart *et al* (Cambridge: Cambridge Univiversity Press) pp 144–69

Pearson R G, Philips S J, Loranty M M, Beck P S A, Damoules T, Knight S J and Goetz S J 2013 Shifts in Arctic vegetation and associated feedbacks under climate change *Nat. Clim. Change* **3** 673–7

Peters G P, Marland G, Quere C L, Boden T A, Canadell J G and Raupach M R 2012 Rapid growth in CO_2 emissions after the 2008–2009 global financial crisis *Nat. Clim. Change* **2** 2–4

Raich J W, Rastetter E B, Melillo J M, Kicklighter D W, Steudler P A, Peterson B J, Grace A L, Moore B and Vorosmarty C J 1991 Potential net primary productivity in South-America—application of a global-model *Ecol. Appl.* **1** 399–429

Randerson J T *et al* 2006 The impact of boreal forest fire on climate warming *Science* **314** 1130–2

Roeckner E 2003 The atmospheric general circulation model ECHAM 5: I. Model description *Max-Planck-Institut für Meteorologie MPI-Report No.* 349 140 p

Roeckner E, Brokopf R, Esch M, Giorgetta M, Hagemann S, Kornblueh L, Manzini E, Schlese U and Schulzweida U 2004 The atmospheric general circulation model ECHAM 5: II. Sensitivity of simulated climate to horizontal and vertical resolution *Max-Planck-Institut für Meteorologie MPI-Report No.* 354 56 p

Rogers B M, Randerson J T and Bonan G B 2013 High-latitude cooling associated with landscape changes from North American boreal forest fires *Biogeosciences* **10** 699–718

Rupp T S, Chapin F S III and Starfield A M 2001 Modeling the influence of topographic barriers on treeline advance at the forest-tundra ecotone in Northwestern Alaska *Clim. Change* **48** 399–416

Rupp T S, Starfield A M and Chapin F S III 2000 A frame-based spatially explicit model of subarctic vegetation response to climatic change- comparison with a point model *Landscape Ecol.* **15** 383–400

Shaver G R and Chapin F S III 1991 Production: Biomass relationships and element cycling in contrasting arctic vegetation *Ecol. Monogr.* **61** 1–31

Shuman J K, Shugart H H and O'Halloran T L 2011 Sensitivity of Siberian larch forests to climate change *Glob. Change Biol.* **17** 2370–84

Sistla S A, Moore J C, Simpson R T, Gough L, Shaver G R and Schimel J P 2013 Long-term warming restructures Arctic tundra without changing net soil carbon storage *Nature* **497** 615–8

Sturm M, Douglas T, Racine C and Liston G 2005 Changing snow and shrub conditions affect albedo with global implications *J. Geophys. Res.* **110** G01004

Sullivan P F, Sommerkorn M, Rueth H M, Nadelhoffer K J, Shaver G R and Welker J M 2007 Climate and species affect fine root production with long-term fertilization in acidic tussock tundra near Toolik Lake, Alaska *Oecologia* **153** 643–52

Suarez F, Binkley D, Kaye M W and Stottlemyer R 1999 Expansion of forest stands into tundra in the Noatak National Preserve, northwest Alaska *Ecoscience* **6** 465–70

Tape K, Sturm M and Racine C 2006 The evidence for shrub expansion in Northern Alaska and the Pan-Arctic *Glob. Change Biol.* **12** 686–702

Turetsky M R, Benscoter B, Page S, Rein G, van der Werf G R and Watts A 2015 Global vulnerability of peatlands to fire and carbon loss *Nat. Geosci.* **8** 11–4

Van Wijk M T, Williams M, Gough L, Hobbie S E and Shaver G R 2003 Luxury consumption of soil nutrients: a possible competitive strategy in above-ground and below-ground biomass allocation and root morphology for slow-growing arctic vegetation? *J. Ecol.* **91** 664–76

Viereck L A 1979 Characteristics of treeline plant communities in Alaska *Holarctic Ecol.* **2** 228–38

Walsh J E, Chapman W L, Romanovsky V, Christensen J H and Stendel M 2008 Global climate model performance over Alaska and Greenland *J. Clim.* **21** 6156–74

Walter Anthony K M *et al* 2014 A shift of thermokarst lakes from carbon sources to sinks during the Holocene epoch *Nature* **411** 452–6

Ward D S, Kloster S, Mahowald N M, Rogers B M, Randerson J T and Hess P G 2012 The changing radiative forcing of fires: global model estimates for past, present, and future *Atmos. Chem. Phys.* **12** 10857–86

Werner R A, Holsten E H, Matsuoka S M and Burnside R E 2006 Spruce beetles and forest ecosystems in south-central Alaska: a review of 30 years of research *Forest Ecol. Manage.* **227** 195–206

Wilmking M, Juday G P, Barber V A and Zald H S 2004 Recent climate warming forces contrasting growth responses of white spruce at treeline in Alaska through temperature thresholds *Glob. Change Biol.* **10** 1724–36

Yi S, McGuire A D, Kasischke E, Harden J, Kristen M, Michelle M and Turetsky M 2010 A dynamic organic soil biogeochemical model for simulating the effects of wildfire on soil environmental conditions and carbon dynamics of black spruce forests *J. Geophys. Res.—Biogeosci.* **115** 15

Yuan F-M, Yi S-H, McGuire A D, Johnson K D, Liang J, Harden J W, Kasischke E S and Kurz W A 2012 Assessment of boreal forest historical C dynamics in the Yukon River Basin: relative roles of warming and fire regime change *Ecol. Appl.* **22** 2091–109

Zhang W, Jansson C, Miller P A, Smith B and Samuelson P 2014 Biogeophysical feedbacks enhance the Arctic terrestrial carbon sink in regional Earth system dynamics *Biogeosciences* **11** 5503–19

Zhu Z and McGuire A D (ed) 2016 Baseline and projected future carbon storage and greenhouse-gas fluxes in ecosystems of Alaska U.S *U.S. Geological Survey Professional Paper 1826* 196 p (doi:10.3133/pp1826)

Zhuang Q, McGuire A D, O'Neill K P, Harden J W, Romanovsky V E and Yarie J 2003a Modeling soil thermal and carbon dynamics of a fire chronosequence in interior Alaska *J. Geophys. Res.—Atmos.* **108** 8147

Zhuang Q, Romanovsky V E and McGuire A D 2001 Incorporation of a permafrost model into a large-scale ecosystem model-Evaluation of temporal and spatial scaling issues in simulating soil thermal dynamics *J. Geophys. Res.—Atmos.* **106** 33649–70

Zhuang Q *et al* 2003b Carbon cycling in extratropical terrestrial ecosystems of the northern hemisphere during the 20th century—a modeling analysis of the influences of soil thermal dynamics *Tellus* B **55** 751–76